Ab initio model potential calculations on the electronic spectrum of Ni^{2+}-doped MgO including correlation, spin–orbit and embedding effects

Rosa Llusar
Departament de Ciènces Experimentals, Universitat Jaume I, Box 242, 12080 Castelló, Spain

Marcos Casarrubios, Zoila Barandiarán, and Luis Seijo[a)]
Departamento de Química Física Aplicada, C-14, Universidad Autónoma de Madrid, 28049 Madrid, Spain

(Received 18 December 1995; accepted 18 June 1996)

An *ab initio* theoretical study of the optical absorption spectrum of Ni^{2+}-doped MgO has been conducted by means of calculations in a MgO-embedded $(NiO_6)^{10-}$ cluster. The calculations include long- and short-range embedding effects of electrostatic and quantum nature brought about by the MgO crystalline lattice, as well as electron correlation and spin–orbit effects within the $(NiO_6)^{10-}$ cluster. The spin–orbit calculations have been performed using the spin–orbit-CI WB-AIMP method [Chem. Phys. Lett. **147**, 597 (1988); J. Chem. Phys. **102**, 8078 (1995)] which has been recently proposed and is applied here for the first time to the field of impurities in crystals. The WB-AIMP method is extended in order to handle correlation effects which, being necessary to produce accurate energy differences between spin–free states, are not needed for the proper calculation of spin–orbit couplings. The extension of the WB-AIMP method, which is also aimed at keeping the size of the spin–orbit-CI within reasonable limits, is based on the use of spin-free-state shifting operators. It is shown that the unreasonable spin–orbit splittings obtained for $MgO:Ni^{2+}$ in spin–orbit-CI calculations correlating only 8 electrons become correct when the proposed extension is applied, so that the same CI space is used but energy corrections due to correlating up to 26 electrons are included. The results of the ligand field spectrum of $MgO:Ni^{2+}$ show good overall agreement with the experimental measurements and a reassignment of the observed $E_g(b^3T_{1g})$ excited state is proposed and discussed. © *1996 American Institute of Physics.* [S0021-9606(96)00836-7]

I. INTRODUCTION

The Ni^{2+}-doped MgO lasing material has been extensively studied using spectroscopic techniques,[1–13] mainly because the Ni^{2+} substitutional defect is in a rigid, highly symmetrical site, which reduces the complications of the spectral analysis and makes it an ideal prototypical system for testing interpretative models of the spectroscopy of Ni^{2+} impurities in sixfold coordination in ionic crystals. Electron paramagnetic resonance,[1] optical absorption and emission,[1–9] magnetic circular dichroism,[10] excited state absorption and excited state emission,[8,11,12] and two-photon excitation[13] experimental studies have been conducted in this material. Theoretical models based on empirical data exist as well.[5,14–16] Consequently, many of the features of the ground and excited local electronic states associated to the Ni^{2+} impurity, which substitutes a Mg^{2+} cation, are known.

The detailed knowledge of most of the spin–orbit components of the ligand field local states in $MgO:Ni^{2+}$ and similar materials is of key importance to understand and predict laser activity. For instance, the location of the ^1E_g and a^3T_{1g} spin–orbit components is important since they are related to the $^3T_{2g}\rightarrow a^3T_{1g}$ excited state absorption (ESA),[8,12] a loss mechanism of the laser emission which can be reduced, in order to gain laser efficiency, by lowering the overlap between the emission and the ESA bands upon cooling. Also, higher ligand field states, like a^1T_{2g}, can be involved in cross relaxation processes which appear at high impurity concentrations and can be used in order to gain laser efficiency.[9] However, as it is well known, no single experimental technique gives nor is expected to give all the information about the whole set of interesting local electronic states; on the contrary, all of them are used, in a complementary way, in order to draw as much information as possible. Along this line, the importance of a close collaboration between experimentation and theory in order to facilitate new achievements in the field of doped materials is openly accepted.[17] In this respect, *ab initio* calculations, which have been shown to provide reliable structural and spectroscopic information for molecules in the gas phase along the years, (sometimes overlapping the experimental one and some times complementing it,) should be of use as another source of complementary information in this kind of solid state materials. This can be expected as a consequence of last years' developments in embedding techniques which allow to include environmental effects into an otherwise isolated cluster with a high degree of reliability.[18]

However, in contrast to the abundance of experimental studies, *ab initio* calculations on the local structure and electronic spectrum of $MgO:Ni^{2+}$ have not been reported to date, to our knowledge.

From the *ab initio* point of view, the spectroscopy of

[a)]Corresponding author; electronic mail: 1s@sara.qfa.uam.es

$MgO:Ni^{2+}$ poses a challenge, since its study requires a balanced description of electron correlation and spin–orbit effects within the cluster formed by the Ni^{2+} impurity and its first O^{2-} coordination shell, as well as of embedding effects brought about to the cluster by the surrounding crystalline lattice. In effect, the importance of *electron correlation* in order to understand the electronic structure of transition metal impurities in ionic crystals is out of the question.[19] Also, the *spin–orbit* splittings are a relevant part of the electronic spectra of Ni^{2+} impurities in ionic crystals[13] and, although in this case the spin–orbit effects could probably be handled by perturbation techniques, they could hardly be neglected. Finally, evidences are being accumulated that *embedding* effects are important for a reliable description of the electronic spectra of this kind of doped solid state materials, both because of their direct effect on the transition energies and because of their indirect effect through the ground and excited states equilibrium structures.[20–22] In particular, the *ab initio* calculation of the absorption spectrum requires the knowledge of the $(NiO_6)^{10-}$ cluster geometry in its ground state; however, although it could be attainable through x-ray-absorption near-edge structure (EXAFS) measurements,[23] it is presently unknown. Moreover, the calculation of the emission spectrum and of excited state absorption spectra requires, in addition, the knowledge of the cluster geometry of excited states,[24] which are not accessible directly by experimental techniques. If these geometries are to be calculated with *ab initio* methods, the use of proper embedding is compulsory.[22,25–27]

The first goal of this paper is to present the results of *ab initio* embedded-cluster calculations on the electronic spectrum of substitutional Ni^{2+} defects in bulk MgO. The calculations have been performed on a $(NiO_6)^{10-}$ cluster which has been embedded in an *ab initio* model potential representation of the MgO lattice according to the prescriptions of Refs. 25 and 28. This embedding incorporates, into the cluster, lattice effects of electrostatic nature [long-range (Madelung) and short-range Coulomb effects] and of quantum nature (exchange and cluster/lattice orthogonality effects). The energies of the ground and excited states of the MgO-embedded $(NiO_6)^{10-}$ cluster have been obtained in complete-active-space self-consistent-field (CASSCF)[29] and average coupled-pair functional (ACPF)[30] calculations, correlating up to 26 valence electrons. Scalar relativistic effects (mass-velocity and Darwin) have been included by means of the Cowan–Griffin-based[31] *ab initio* core model potential method, CG-AIMP.[32,33] Spin–orbit relativistic effects have been incorporated through the Wood–Boring-based[34] AIMP method, WB-AIMP, which has been recently proposed as a means to reliably and economically include spin–orbit effects in *ab initio* molecular calculations.[35,36]

The second goal of this paper is to propose and use a further development of the WB-AIMP method,[36] designed in order to improve the spin–orbit couplings between spin-free states. In effect, a good description of the relative energy of the spin-free states is necessary in order to properly describe the spin–orbit splittings in *ab initio* calculations in systems where spin–orbit is not a very small perturbation. This description often requires large multiconfigurational expansions. Some authors handle this problem by building a spin–orbit-CI matrix on a small basis of spin–free CI wave functions (usually several hundreds) which already includes as much electron correlation as possible;[37] then, perturbation techniques are used to include the effects of the remaining configurations both in spin–orbit and electron correlation effects. On the other hand, in spin–orbit methods in which the electron repulsion and spin–orbit operators are simultaneously included in the spin–orbit-CI matrix,[38,39] as it is the case of the WB-AIMP method used here,[36] the inclusion of the necessary correlation effects leads very often to unmanageable large CI matrices. We propose and use, in this paper, a simple and efficient technique, based on the use of spin-free-state shifting operators, aimed at correcting for correlation effects not considered at the spin–orbit-CI level, while keeping the size of the CI matrix manageable. It is shown here that, while spin–orbit-CI calculations correlating only 8 electrons of the $(NiO_6)^{10-}$ cluster lead to wrong spin–orbit splittings, these are corrected by the proposed technique in spin–orbit-CI calculations of the same size; this success is achieved by incorporating corrections resulting from spin-free calculations correlating 26 cluster valence electrons.

In Sec. II we summarize the method used for the present calculations and describe the proposed extension of the WB-AIMP method, as well as details of the calculations. The results are discussed in Sec. III and the conclusions appear in Sec. IV.

II. METHOD AND DETAILS OF THE CALCULATIONS

The optical spectrum of Ni^{2+}-doped MgO is mainly due to Ni^{2+} impurities which substitute Mg^{2+} ions in the center of an octahedron of O^{2-} ions. It corresponds to transitions between spin–orbit components of electronic states localized in the Ni^{2+} impurities and in their first coordination shell of O^{2-}, which are mainly affected by the bonding interactions between these ions but also influenced by the environmental effects brought about by the rest of the MgO ionic lattice. Consequently, we performed *ab initio* calculations in several low lying electronic states of a MgO-embedded $(NiO_6)^{10-}$ cluster, which include intracluster electron correlation and spin–orbit interactions, as well as electrostatic and quantum environmental effects on the cluster. Next we summarize the methods used for this embedded cluster calculations.

A. The AIMP embedding technique

In this subsection, we summarize the main features of the *ab initio* model potential embedding technique used here, which is a practical implementation of the group function theory developed by McWeeny[40] (in the context of intermolecular interactions) and Huzinaga[41] (in the context of frozen-core molecular calculations) to the study of local properties of imperfect crystals. It has been presented in Refs. 25 and 28 for *ab initio* calculations on clusters embedded in unpolarized, unrelaxed, frozen ionic lattices, and extended in Ref. 27 in order to embed clusters, when necessary,

in relaxed, dipole polarized ionic lattices, making use of the empirical shell-model description of the lattice.[42]

Assuming that the local structure and the ligand-field absorption/emission electronic transitions in Ni^{2+}-doped MgO are dominated by the interactions within a $(NiO_6)^{10-}$ unit (*cluster*) including electron correlation and spin–orbit effects, and by nondynamical quantum mechanical interactions between this unit and the rest of the ionic lattice (*environment*) such as long- and short-range Coulomb, exchange, and orthogonality interactions, and that they should not be affected by correlation effects between the $(NiO_6)^{10-}$ cluster and the environment, a good approximation for the wave function of the imperfect crystal local states is, according to McWeeny[40]

$$\Psi_{MgO:Ni^{2+}} = M\hat{A}[\Phi_{(NiO_6)^{10-}}\Phi_{Mg^{2+}}\ldots\Phi_{O^{2-}}\ldots], \qquad (1)$$

where M is a normalization constant, $\hat{A}$ is an intergroup antisymetrizer, $\Phi_{(NiO_6)^{10-}}$ is the antisymmetric embedded-cluster wave function, describing N_{clus} electrons, which can be any suitable mono- or multiconfigurational expansion, and $\Phi_{Mg^{2+}}$, $\Phi_{O^{2-}}$ are wave functions describing all the Mg^{2+} and O^{2-} components of the environmental crystalline lattice. This approximation leads, when the embedded group functions are strong-orthogonal,[40] to a partitioning of the crystal total energy in terms of environment energy, cluster energy and interaction energy between cluster and environment. The last two terms include all the direct dependencies on the cluster nuclei and wave function, and read

$$\begin{aligned} &E_{(NiO_6)^{10-}} + E_{(NiO_6)^{10-}-\mathrm{env}} \\ &= \sum_{\alpha}^{(NiO_6)^{10-}} \sum_{\mu}^{\mathrm{env}} \frac{Z_\alpha Z_\mu}{R_{\alpha\mu}} \\ &\quad + \sum_{\alpha}^{(NiO_6)^{10-}} \sum_{\mu}^{\mathrm{env}} \langle\Phi_\mu| - \sum_{i\epsilon\mu} \frac{Z_\alpha}{r_{\alpha i}} |\Phi_\mu\rangle \\ &\quad + \langle\Phi_{(NiO_6)^{10-}}|\hat{H}_{\mathrm{emb}-(NiO_6)^{10-}}|\Phi_{(NiO_6)^{10-}}\rangle, \end{aligned} \qquad (2)$$

where α runs over the cluster nuclei, μ runs over the environmental ions, i runs over μ's electrons, the first term in the right hand side is the repulsion between nuclei in the cluster and in the environment, the second is the attraction between the cluster nuclei and the environmental electrons, and the third one is the interaction between the cluster electrons and the entire crystal, $\hat{H}_{\mathrm{emb}-(NiO_6)^{10-}}$ being the embedded-cluster Hamiltonian.

The two first terms in the right hand side of Eq. (2) are simple to calculate once frozen wave functions for the environmental ions are known. Minimizing the third term leads to the variational embedded-cluster wave function $\Phi_{(NiO_6)^{10-}}$. In order to do so, we use the restricted space variational method of Huzinaga[41] and, in addition, we adopt the AIMP approximation for environmental Coulomb and exchange operators;[25,28] in this way, the variational procedure is performed simply by using standard molecular *ab initio* methods, (in this paper they are CASSCF[29] and ACPF[30] calculations including spin-free relativistic effects by means of the Cowan–Griffin based *ab initio* model potential method CG-AIMP,[32,33] as well as spin–orbit-CI[39] calculations including in addition spin–orbit effects by means of the WB-AIMP method[36]) and the following embedded-cluster Hamiltonian

$$\begin{aligned} \hat{H}_{\mathrm{emb}-(NiO_6)^{10-}} &= \hat{H}_{\mathrm{isolated}-(NiO_6)^{10-}} \\ &\quad + \sum_{i}^{(NiO_6)^{10-}} \sum_{\mu}^{\mathrm{env}} [V_\mu^{\mathrm{lr}}(i) + V_\mu^{\mathrm{sr}}(i)]. \end{aligned} \qquad (3)$$

Here, $V_\mu^{\mathrm{lr}}(i)$ is the long-range embedding potential originated by the lattice ion μ on the cluster electron i, which is in this paper

$$V_\mu^{\mathrm{lr}}(i) = -\frac{Q_\mu}{r_{\mu i}}, \qquad (4)$$

Q_μ being the ionic charge ($Q_{Mg^{2+}} = +2$, $Q_{O^{2-}} = -2$,) located at the lattice ionic sites, and the corresponding short-range embedding potential is

$$\begin{aligned} V_\mu^{\mathrm{sr}}(i) &= \sum_k \frac{C_k^\mu \exp(-\alpha_k^\mu r_{\mu i}^2)}{r_{\mu i}} \\ &\quad + \sum_l \sum_{m=-l}^{+l} \sum_{a,b} |alm;\mu\rangle A_{l;ab}^\mu \langle blm;\mu| \\ &\quad + \sum_c (-2\varepsilon_c^\mu) |\phi_c^\mu\rangle\langle\phi_c^\mu|. \end{aligned} \qquad (5)$$

The first term in the right hand side of Eq. (5) is the short-range Coulomb model potential originated by the environmental ion μ; its parameters C_k^μ and α_k^μ in an arbitrary number, are calculated by a least-square fitting to the true short-range Coulomb potential, $(Q_\mu - Z_\mu)/r_{\mu i} + \hat{J}_\mu(r_{\mu i})$, $\hat{J}_\mu$ being the one-electron Coulomb operator associated to the many-electron wave function of ion μ, Φ_μ. The second term is the exchange model potential of ion μ; it is the spectral representation of the negative of its true exchange operator, $-\hat{K}_\mu$, on the subspace defined by the set of primitive Gaussian functions $|alm;\mu\rangle$ used in the expansion of its occupied orbitals, ϕ_c^μ In consequence, the $A_{l;ab}^\mu$ coefficients are the elements of the matrix $\underline{A}^\mu$ resulting from the transformation

$$\underline{A}^\mu = -(\underline{S}^\mu)^{-1}\underline{K}^\mu(\underline{S}^\mu)^{-1}, \qquad (6)$$

where $\underline{S}^\mu$ is the overlap matrix on the quoted subspace, and $\underline{K}^\mu$ is the matrix of $\hat{K}_\mu$ in the same subspace. The third term in the right hand side of Eq. (5) is the projection operator of ion μ, originated by the restricted variational treatment,[41] which is responsible for preventing the collapse of the cluster wave function onto the environmental ion μ; ε_c^μ is the orbital energy of the embedded orbital ϕ_c^μ, and the index c runs over the occupied orbitals. As corresponding to the AIMP main idea,[43] all three terms in Eq. (5) are calculated directly from known ϕ_c^μ orbitals without resorting to any kind of parametrization procedure in terms of a reference, such as those followed in pseudopotential theory. In order to

produce all the necessary data for the short-range embedding model potentials [Eq. (5)], a preliminary *self-consistent-embedded-ions* calculation, SCEI, is performed on perfect MgO, consisting on an iterative series of embedded-Mg^{2+} and embedded-O^{2-} SCF calculations with the respective embedding potentials located at perfect MgO lattice experimental sites[44] [$a_0 = 4.2112$ Å]. The SCEI calculation on MgO leads to the embedded Mg^{2+} and O^{2-} occupied orbitals and orbital energies, $\{\phi_c^{Mg^{2+}} \ \varepsilon_c^{Mg^{2+}}\},\{\phi_c^{O^{2-}} \ \varepsilon_c^{O^{2-}}\}$, which is all the information necessary to produce the embedding potentials; it has been performed in Ref. 26 and the detailed data are available from the authors.[45]

B. The cluster Hamiltonian

We use core *ab initio* model potentials[32,33,36,43] for the cluster components, so that the isolated cluster Hamiltonian contribution to Eq. (3) may be written

$$\hat{H}_{\text{isolated}-(NiO_6)^{10-}} = \sum_i^{N_{\text{val}}} h(i) + \sum_{i>j}^{N_{\text{val}}} \frac{1}{r_{ij}}, \tag{7}$$

where N_{val} is the number of valence electrons in the $(NiO_6)^{10-}$ cluster, with the one-electron contribution being, in general,

$$h(i) = -\tfrac{1}{2}\Delta_i - \frac{(Z^{\text{Ni}} - Z^{\text{Ni}}_{\text{core}})}{r_{\text{Ni},i}} + V^{\text{Ni}}_{\text{core}-\text{AIMP}}(i) + \sum_I^{O_6}\left[-\frac{(Z^{\text{O}} - Z^{\text{O}}_{\text{core}})}{r_{I,i}} + V^{\text{O}}_{\text{core}-\text{AIMP}}(i)\right]. \tag{8}$$

Here, $Z^{\text{Ni}}_{\text{core}}$ and $Z^{\text{O}}_{\text{core}}$ are the number of core electrons of nickel and oxygen which are arbitrarily frozen, and $V^{\text{Ni}}_{\text{core-AIMP}}(i)$ and $V^{\text{O}}_{\text{core-AIMP}}(i)$ are the respective one-electron core *ab initio* model potentials. These are

$$V^I_{\text{core}-\text{AIMP}}(i) = \sum_k \frac{C^I_k \exp(-\alpha^I_k r^2_{I,i})}{r_{I,i}} + \sum_l \sum_{m=-l}^{+l} \sum_{a,b} |alm;I\rangle A^I_{l;ab} \langle blm;I| + \sum_c (-2\varepsilon^I_c)|\phi^I_c\rangle\langle\phi^I_c| + \lambda^I \sum_{nl}^{I-\text{valence}} \sum_k \frac{B^{nl,I}_k \exp(-\beta^{nl,I}_k r^2_{I,i})}{r^2_{I,i}} \times \hat{O}_l \hat{l}\hat{s}\hat{O}_l, \tag{9}$$

with

$$\hat{O}_l = \sum_{m=-l}^{+l} |lm\rangle\langle lm|. \tag{10}$$

The first three terms of the right hand side of Eq. (9), which are the spin-free part of the core AIMP, are calculated using the whole set of chosen atomic *core* orbitals, $\{\phi^I_c\}$, in exactly the same way as the components of Eq. (5) are obtained from the whole set of *environmental ion* orbitals, with the only exception that the $|alm;I>$ set is now the one formed by all the primitive Gaussian functions used in the valence-only embedded-cluster calculation which are centered on nucleus I. If the source of core orbitals is an atomic nonrelativistic Hartree–Fock calculation, the result is a nonrelativistic core AIMP. If the source is an atomic relativistic Cowan–Griffin–Hartree–Fock calculation[31] instead, the result is a spin-free relativistic CG-AIMP; in this case, however, the coefficients in the second term are rather calculated by means of

$$\underline{A}^I = (\underline{S}^I)^{-1}\{-\underline{K}^I + \underline{V}^I_{\text{mv+Dw}}\}(\underline{S}^I)^{-1}, \tag{11}$$

where $\underline{V}^I_{\text{mv+Dw}}$ is the matrix of the relativistic mass-velocity and Darwin potentials[31,36] corresponding to the valence of atom I on the basis of the $|alm;I\rangle$ primitives.

The fourth term in the right hand side of Eq. (9) is the spin–orbit component of the model potential, WB-AIMP.[36] It is evaluated using all the orbitals resulting from a relativistic Cowan–Griffin–Hartree–Fock atomic calculation and it is added to the spin-free relativistic CG-AIMP.

C. The spin-free-state-shifted cluster Hamiltonian

It is known that a good description of the relative energy of the spin-free states of a given system [say $\Phi(iSM_S\Gamma\gamma)$, i being an ordinal number, S, M_S the spin quantum numbers and Γ, γ the spatial point group irreducible representation and subspecies, respectively,] is necessary in order to reliably describe spin–orbit splittings in *ab initio* spin–orbit-CI kind of calculations.[37] This requires very often the inclusion of large amounts of electron correlation at the same time that spin–orbit effects, which poses major problems to spin–orbit-CI algorithms[39] since the symmetry breaking leads to much larger matrices than those required in spin-free-CI algorithms. As a consequence, spin–orbit-CI calculations are in practice much more restricted than spin-free-CI calculations in terms of electron correlation.

On the other hand, whereas the size of the spin–orbit effects is governed by two factors, namely, the size of the spin–orbit couplings between the $\Phi(iSM_S\Gamma\gamma)$ states and their energy differences, one can expect that they both demand a different degree of quality in the spin-free wave functions. In particular, a CI space $\mathscr{S}$ leading to a set of $\Phi^{\mathscr{S}}(iSM_S\Gamma\gamma)$ spin-free-CI wave functions, with spin-free eigenvalues $E^{\mathscr{S}}(iS\Gamma)$, which are good enough for the calculation of the spin–orbit couplings could not be sufficient to attain a similarly good description of the spin-free electronic spectrum, which could eventually be very demanding in terms of electron correlation effects and require a larger CI space, say $\mathscr{R}$. Let us call $\Phi^{\mathscr{R}}(iSM_S\Gamma\gamma)$ the spin-free wave functions meeting the latter requirements and $E^{\mathscr{R}}(iS\Gamma)$ their corresponding eigenvalues. Under these circumstances, it could be a reasonable solution to use the simpler $\Phi^{\mathscr{S}}(iSM_S\Gamma\gamma)$ CI wave functions to calculate the spin–orbit couplings and the more sophisticated $\Phi^{\mathscr{R}}(iSM_S\Gamma\gamma)$ ones to calculate the spin-free energy differences. This could

be achieved simply by using the smaller CI space $\mathscr{S}$ and the following Hamiltonian, which we may call a spin-free-state-shifted spin–orbit Hamiltonian,

$$\hat{H}^{\mathrm{sfss}}_{\mathrm{emb}-(\mathrm{NiO_6})^{10-}} = \hat{H}_{\mathrm{emb}-(\mathrm{NiO_6})^{10-}} + \sum_{iSM_S\Gamma\gamma} \delta(iS\Gamma) \times |\Phi^{\mathscr{S}}(iSM_S\Gamma\gamma)\rangle\langle\Phi^{\mathscr{S}}(iSM_S\Gamma\gamma)|, \quad (12)$$

$\hat{H}_{\mathrm{emb}-(\mathrm{NiO_6})^{10-}}$ being that in Eq. (3) and

$$\delta(iS\Gamma) = [E^{\mathscr{R}}(iS\Gamma) - E^{\mathscr{R}}(\mathrm{G.S.})] - [E^{\mathscr{S}}(iS\Gamma) - E^{\mathscr{S}}(\mathrm{G.S.})], \quad (13)$$

where $E^{\mathscr{R}}$(G.S.) and $E^{\mathscr{S}}$(G.S.) are the spin-free-CI energies of a common given state (usually the ground state) corresponding to the $\mathscr{R}$ and $\mathscr{S}$ CI spaces, respectively. This Hamiltonian, if the spin–orbit operator is neglected, leads within the CI space $\mathscr{S}$ to the $\Phi^{\mathscr{S}}(iSM_S\Gamma\gamma)$ wave functions but to the $[E^{\mathscr{R}}(iS\Gamma) - E^{\mathscr{R}}(\mathrm{G.S.})]$ energy differences, that is, to spin-free wave functions and energy differences of the desired quality for a proper calculation of spin–orbit splittings. Eq. (12) requires the knowledge of the $E^{\mathscr{R}}(iS\Gamma) - E^{\mathscr{R}}(\mathrm{G.S.})$ values; they may be calculated by means of spin-free methods able to take full advantage of the spin symmetry and capable of handling the CI space $\mathscr{R}$, supposedly unreachable by the spin–orbit-CI technique in use. (Alternatively, they could be taken from experimental data if the spin–orbit contributions could be removed by an averaging procedure, which is sometimes possible, but often full of arbitrariness and not very reliable.[46]) The set $\Phi^{\mathscr{S}}(iSM_S\Gamma\gamma)$ and $E^{\mathscr{S}}(iS\Gamma)$ can be calculated either in a preliminary run of the spin–orbit-CI codes neglecting the spin–orbit operator or by using a spin-free-CI code.

In practice, the sum on Eq. (12) must be limited to a small number of spin-free states which would depend on the particular problem; it seems reasonable to think that they must include all the sates of interest and those above them within a chosen energy threshold. In this paper we extend it to all the spin-free states resulting from the configurations $t_{2g}^x e_g^y, x+y=8, t_{2g}$ and e_g being the molecular orbitals of the $(\mathrm{NiO_6})^{10-}$ cluster with main character Ni($3d$).

We would like to mention here that the details of this method, proposed in order to improve the quality of the computed spin–orbit splittings while limiting the calculations to manageable CI spaces, are different to the ones of the CIPSO method proposed by Teichteil *et al.*,[37] and that the meaning of the corrections are not fully equivalent. However, the idea behind the use of the spin-free-state-shifted Hamiltonian proposed here is exactly the one in Ref. 37.

D. Details of the calculations

All the calculations presented in this paper are performed on a $(\mathrm{NiO_6})^{10-}$ cluster embedded in a set of 722 Mg^{2+} and O^{2-}m AIMP embedding potentials described in Sec. II A, which lie within a cube of length equal to four unit cells ($4\ a_0$) centered on the Ni^{2+} impurity. Those of them located within cubic shells of length larger than $2\ a_0$ contribute only with the long-range point-charge potential, $V_\mu^{\mathrm{lr}}(i)$. The ones on the cube edges contribute with fractional charges.[47] On the sites of the Mg^{2+} nearest-neighbors of the cluster oxygens we include always a (10/4) basis set[26] which facilitates achieving a high degree of cluster/environment orthogonality.

TABLE I. Spin–orbit potentials for Ni [last term in Eq. (9)].

	3p potential		3d potential	
k	β_k^{3p}	B_k^{3p}	β_k^{3d}	B_k^{3d}
1	4321700.0	0.325570978	3204800.0	0.348767139
2	375000.0	0.298132105	268000.0	0.284375931
3	34800.0	0.143107623	23470.0	0.126054238
4	3650.0	0.0527378123	2320.0	0.0436529692
5	396.0	0.0184504630	241.9	0.0148858946
6	42.2	0.00647186996	25.79	0.00482056596
7	3.83	0.00182057286	2.640	0.00141152641
8	0.396	0.000231128715	0.227	0.000124829754

In a first series of nonrelativistic calculations we adopted an all-electron approximation for nickel ($Z^{\mathrm{Ni}}_{\mathrm{core}}=0$, $V^{\mathrm{Ni}}_{\mathrm{core-AIMP}}=0$,) with the ($14s11p5d$) Gaussian basis set of Wachters[48] augmented with one d-type diffuse function[49] and a ($3f$) polarization function[50] contracted as (62111111/4211111/3111/3), and a [He]–core nonrelativistic AIMP approximation for the oxygens ($Z^{\mathrm{O}}_{\mathrm{core}}=2$, $V^{\mathrm{O}}_{\mathrm{[He]-CG-AIMP}}$,) with core AIMP and valence basis set taken from Ref. 43, the latter augmented with one diffuse p function for the anion[51] and contracted as (41/411). This description has been used in Ref. 18, where the nickel–oxygen bond distance, $r_e(\mathrm{Ni-O})$, has been optimized in CASSCF calculations on the $^3A_{2g}$ ground state of the embedded $(\mathrm{NiO_6})^{10-}$ cluster, using 8 electrons in an active space defined by the t_{2g} and e_g molecular orbitals with main character Ni($3d$), the result being $r_e(\mathrm{Ni-O})=2.144$ Å .

Using the optimized local structure and the same basis sets, we have calculated the nonrelativistic ligand field absorption spectrum including electron correlation effects by means of the approximately size-consistent ACPF method, using the same active space as in the CASSCF calculation and correlating 26 electrons, 16 occupying the molecular orbitals resulting from the CASSCF($^3A_{2g}$) calculation of main character Ni($3s,3p,3d$), plus 10 in the outermost closed shells t_{2g} and e_g of main character O($2p$), which corresponds to the recommendations by Pierloot and Vanquickenborne[52] for ligand field transitions in this kind of systems. We will refer to these spin-free calculations as ACPF-26. They have been performed using the MOLCAS-2 package[53] for molecular electronic structure calculations and the ECPAIMP program[54] for evaluating the AIMP integrals.

In a second series of relativistic spin–orbit-CI calculations, aimed at calculating the ligand field spectrum including spin–orbit effects, we adopted a [Mg]–core spin–orbit WB-AIMP approximation for nickel and the same [He]-core nonrelativistic AIMP approximation for the oxygens as before. For Ni, all the spin-free components of the relativistic core AIMP correspond to Ref. 33 (the CG-AIMP part) and the spin–orbit potential parameters have been obtained for

TABLE II. Spin–orbit-corrected minimal valence basis set of Ni (prior to splitting) used in the relativistic spin-free CG-AIMP and spin–orbit WB-AIMP calculations.

Exponent	Coefficient	Exponent	Coefficient
4s		3p	
5.08964646E+03	−1.25122206E−03	3.46842038E+02	−1.94185728E−02
7.25751102E+02	−8.58410158E−03	7.98503855E+01	−1.05917399E−01
1.58290395E+02	−2.69169868E−02	2.39713184E+01	−2.52521503E−01
1.48525706E+01	1.20534022E−01	2.88500165E+00	6.24008854E−01
5.35630309E+00	7.59918568E−02	9.53255566E−01	4.69164452E−01
2.68841156E+00	−2.00503005E−01	3d	
9.96402768E−01	−2.96500796E−01	4.72987287E+01	3.07988156E−02
1.26351512E−01	6.22597831E−01	1.31525058E+01	1.54011592E−01
4.48261888E−02	5.07154907E−01	4.40653743E+00	3.74829411E−01
		1.46981906E+00	4.72616234E−01
		4.33897325E−01	3.13307183E−01
Added functions			
p			
0.111	1.0000000		
d			
0.1316	1.0000000		
f			
6.7446890	0.1737857		
2.4188007	0.5973381		
1.0357592	0.3929396		

this work and they are presented in Table I. The valence basis sets are as well those in Ref. 33, extended with the same functions as in the nonrelativistic calculation, and with the innermost coefficient of the $3p$ and $3d$ orbitals corrected according to Ref. 36 so that the spin–orbit atomic coupling constants are correctly calculated while the properties depending on the outer parts of the orbitals remain untouched; the so called spin–orbit-corrected basis set which results for Ni is presented in Table II. For oxygen, a (41/41) valence basis set was used, in which the outermost s exponent and the two outermost p ones, as well as all the coefficients, have been optimized in MgO-embedded O^{2-} SCF calculations; this has been done in order to reduce the size of the cluster basis set while keeping its ability to represent the anion electron density.

These spin–orbit-CI calculations have been performed using the same reference space as in the nonrelativistic ACPF-26 calculations, and including all single and double excitations from the mainly-Ni($3d$) orbitals, all single excitations from the mainly-Ni($3p$) orbitals and the double excitations Ni($3p$)→Ni($3d$), which are known to play an important role in the relative term energies of the $3d^n$ configurations of first-row transition metal atoms and, in particular, in Ni^{2+}.[55] The molecular orbitals correspond to a restricted-Hartree–Fock calculation on the average state $(E(^3A_{2g})+E(^3T_{2g}))/2$. We will refer to these spin–orbit-CI calculations as WB-AIMP CI($3d^8$-SD*). This kind of CI space, which is in the line of the specific-CI spaces for transition energies proposed by Miralles *et al.*,[56] is in the edge of what we are presently able to manage with the spin–orbit-CI code based on double-group symmetry adapted functions,[57] but it is however rather more limited than the spin-free ACPF-26 calculations. In order to handle at a time the correlation effects included in the ACPF-26 calculation and the spin–orbit effects included in the WB-AIMP CI($3d^8$-SD*) one, we performed spin-free-state-shifted WB-AIMP calculations, sfss-WB-AIMP CI($3d^8$-SD*); in these, the $\mathscr{R}$ level of calculation in Eq. (13) is ACPF-26, the $\mathscr{S}$ level is the one resulting from neglecting the spin–orbit operator in the WB-AIMP CI($3d^8$-SD*) calculation, which we call CG-AIMP CI($3d^8$-SD*), and the sum in Eq. (12) extends to all the spin-free states resulting from the main configurations $(t_{2g},e_g)^8$.

III. RESULTS AND DISCUSSION

The results of the spin-free ligand field absorption spectrum computed using the optimized local structure of the $(NiO_6)^{10-}$ embedded cluster[18] are presented in Table III as well as in the first and last columns in Fig. 1. Our best spin-free calculation, nonrelativistic ACPF-26, is used as a reference for the calculation of the $\delta(iS\Gamma)$ shifting factors, Eq. (13), also presented in Table III. These $\delta(iS\Gamma)$, according to Eq. (12), will correct the relative energies of the spin-free CG-AIMP states when they mix in the WB-AIMP calculation as a consequence of the spin–orbit operator. The main effects of the ACPF-26 calculation compared to the simpler CI($3d^8$-SD*) one is reversing the order of the lowest $^3T_{1g}$ and ^1E_g, as well as that of the higher $^3T_{1g}$ and $^1A_{1g}$; these effects will have a significant consequence in the spin–orbit splittings, as we comment below. In Table III we can compare our ACPF-26 calculation with the experimental optical Franck–Condon broadband absorptions measured by Low.[1] The first four bands ($^3A_{2g}\rightarrow{}^3T_{2g}, a^1E_g, a^3T_{1g}, a^1T_{2g}$) have been the object of further experimental studies and their fine structures have been analyzed. The b^3T_{1g} state at 24 500

TABLE III. Spin-free ligand field absorption spectrum of Ni^{2+}-doped MgO. All numbers in cm^{-1}.

$^3A_{2g}\rightarrow$	CG-AIMP CI($3d^8$-SD*)	Nonrelativistic ACPF-26	Experiment[a]	$\delta(iS\Gamma)$[b]
$\rightarrow {}^3T_{2g}$	7290	7960	8600	670
$\rightarrow a^1E_g$	17602	13282	13400	−4320
$\rightarrow a^3T_{1g}$	12486	14141	14800	1655
$\rightarrow a^1T_{2g}$	23993	22172	21550	−1821
$\rightarrow a^1A_{1g}$	27840	24367	[25950]	−3473
$\rightarrow b^3T_{1g}$	25899	27107	[24500]	1208
$\rightarrow {}^1T_{1g}$	30443	29310	28300	−1133
$\rightarrow b^1E_g$	34992	36552	~34500	1560
$\rightarrow b^1T_{2g}$	35631	36767	~34500	1136
$\rightarrow b^1A_{1g}$	63725	61526	–	−2199

[a]Franck–Condon broad band absorptions. Values and assignments from Ref. 1. Assignments in braces are questioned in the text.
[b]Equation (13).

cm^{-1} above the $^3A_{2g}$ ground state has been also observed in ESA[11] and two-photon excitation[13] experiments, which adopted Low's assignments. The a^1A_{1g} state has not been measured again, to our knowledge. The same is true for the rest of the excited states. Our results agree fairly well with the measurements, the deviations being very reasonable and growing up towards larger energies in accordance with a poorer description of the correlation effects in the higher states. The a^1A_{1g} and b^3T_{1g} states are the only exceptions, showing larger deviations and the opposite ordering. Since there is no apparent reason for this strange behavior, we think that the assignments of these two bands should be reversed (we will further justify this below), in which case the overall agreement remains good and the exceptions disappear.

The results of the spin–orbit ligand field absorption spectrum computed by means of the WB-AIMP method using the CI($3d^8$-SD*) wave functions are presented in Table IV and in Fig. 1 together with the experimental results, where we use O_h double group notation and we drop the *gerade* subindex for simplicity. It can be observed that the raw WB-AIMP CI($3d^8$-SD*) calculation leads to unreasonable spin–orbit splittings, which are summarized in the wrong ordering of the A_1, T_1, T_2, E components of the

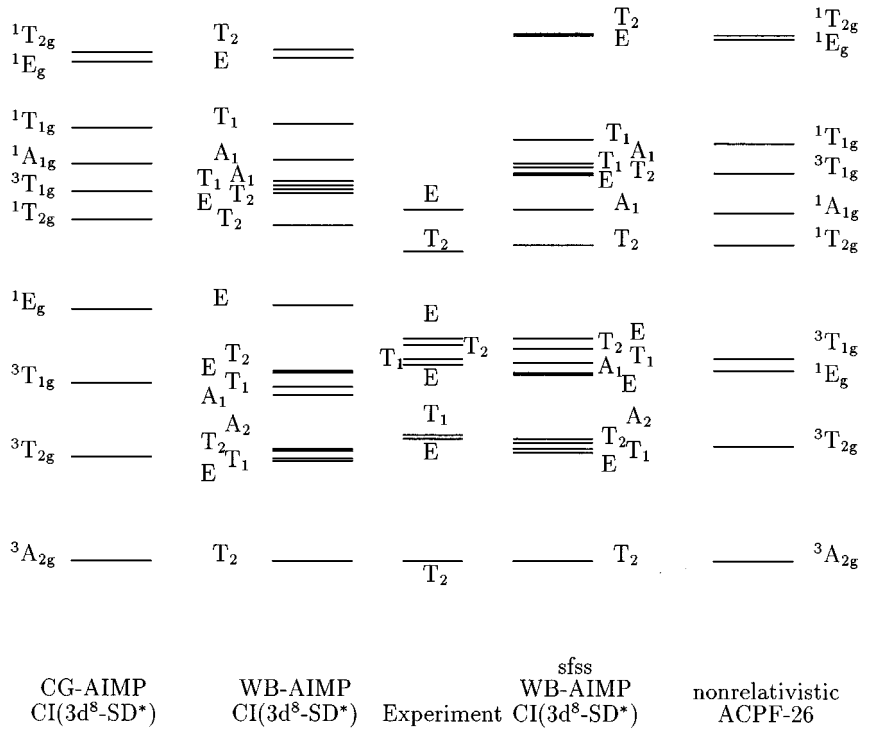

FIG. 1. Ligand field absorption spectrum of Ni^{2+}-doped MgO.

TABLE IV. Spin–orbit ligand field absorption spectrum of Ni^{2+}-doped MgO. All numbers in cm^{-1}. Main spin-free character in parentheses. All states are *gerade*.

$T_2(^3A_2)\rightarrow$	WB-AIMP CI($3d^8$-SD*)	sfss-WB-AIMP CI($3d^8$-SD*)	Experiment[a]
$\rightarrow E\ (^3T_2)$	6 967	7 607	8 605
$\rightarrow T_1\ (^3T_2)$	7 161	7 836	8 783
$\rightarrow T_2\ (^3T_2)$	7 670	8 326	
$\rightarrow A_2\ (^3T_2)$	7 839	8 498	
$\rightarrow E\ (^1E, a^3T_1)$	$E\ (^1E)$ 17 978	12 995	13 650
$\rightarrow A_1\ (a^3T_1)$	11 563	13 187	
$\rightarrow T_1\ (a^3T_1)$	12 225	13 847	14 111
$\rightarrow T_2\ (a^3T_1)$	13 252	14 871	15 150
$\rightarrow E\ (a^3T_1, ^1E)$	$E\ (a^3T_1)$ 13 162	15 516	15 580
$\rightarrow T_2\ (^1T_2)$	23 558	22 111	21 734
$\rightarrow A_1\ (^1A_1)$	28 096	24 579	[ ]
$\rightarrow E\ (b^3T_1)$	25 807	26 972	[24 587]
$\rightarrow T_2\ (b^3T_1)$	26 391	27 218	
$\rightarrow T_1\ (b^3T_1)$	26 427	27 621	
$\rightarrow A_1\ (b^3T_1)$	26 648	27 893	
$\rightarrow T_1\ (^1T_1)$	30 651	29 519	
$\rightarrow E\ (^1E)$	35 219	36 765	
$\rightarrow T_2\ (^1T_2)$	35 843	36 969	
$\rightarrow A_1\ (^1A_1)$	64 005	61 811	

[a]Fine structure Franck–Condon centers. Values and assignments from Ref. 13. Assignments in braces are questioned in the text.

a^3T_1, as a consequence of the wrong relative location of the a^3T_1 and ^1E spin-free states. When this is solved by the use of the spin-free-state shifting technique, sfss-WB-AIMP CI($3d^8$-SD*), the order of states turns out to be correct and the overall description of the spin–orbit components is good. In effect, although the spin–orbit splittings are overestimated as a rule, the relative location of the states is well described and the one to one correspondence between the theoretical energies and the experimental ones is more than reasonable. The largest deviation (2400 cm^{-1}) is in the $E(b^3T_1)$ state, the only observed spin–orbit component of the b^3T_1.

We should mention now that the analysis by Campochiaro *et al.*[13] of the results of the two-photon excitation measurements, whose selection rules for single frequency experiments allow to observe spin–orbit components of all of the excited states as well as to distinguish different components by means of their different polarization, was able to interpret the long-known spectrum in much detail. In consequence, we do not comment here on all the previous studies facing the assignment problem, and we rather refer only to Campochiaro's *et al.* work,[13] which represents the present status of the assignments of the ligand field states in MgO:Ni^{2+}. According to Ref. 13, all of the assignments which have been made are rather unquestionable, except for the one to the components of the b^3T_1, which has been stated as ''puzzling'' by the authors, since the zero-phonon line at 23 897 cm^{-1} (Franck–Condon center at 24 587 cm^{-1}) shows a polarization which is in agreement with an assignment to an E state, but no lines appear at slightly higher energies in spite of the fact that one would expect to see the T_1 and T_2 components as well according to the selection rules.[13] The authors suggest as a possible explanation that the proximity to a charge-transfer transition could broaden the higher-energy features.[13] In this respect, our calculations suggest the possibility that the 24 587 cm^{-1} absorption corresponds to the $A_1(^1A_1)$ component. This possibility is in agreement with its polarization, since both $T_2\rightarrow A_1$ and $T_2\rightarrow E$ show the same one. But at the same time it would explain the fact that no feature is observed in its nearby higher-energy side, since the next state, the $E(^3T_1)$, would appear some 1500–2000 cm^{-1} above it, perhaps masked by the charge-transfer transition. (Note that Low's reported band at 24 500 cm^{-1}[11] should correspond, according to this interpretation, to the $^1A_1$ state, but he also reports another one at $\sim$25 950 cm^{-1} which could be due to the components of the b^3T_1.) We must note that the assignment suggested by our *ab initio* calculations may hardly originate from much simpler crystal field theory calculations performed by several authors,[1,3,10,13] which tend to predict the $^1A_1$ state to be very close to the $^1T_2$ if the relative location of ^1E and a^3T_1 which is observed in this case has to be fulfilled. The weak point of our suggestion, based only on energy difference arguments, comes from the relative intensities in the two-photon excitation experiments, since the intensity calculations by

Campochiaro *et al.*[13] lead to a negligible value for the $A_1(^1A_1)$ absorption, which runs against the suggested assignment. In this respect, we may comment that the intensities calculated in Ref. 13 for the $A_1(^1A_1)$ peak are very similar to the ones for $E(^3T_2)$, both of them much less intense than the components of the a^3T_1, in consistency with the fact that both $^3A_2 \rightarrow {}^1A_1$ and $^3A_2 \rightarrow {}^3T_2$ two-photon transition are forbidden without spin–orbit coupling; however the $E(^3T_2)$ was undoubtfully observed, so that the possibility of the $A_1(^1A_1)$ being observed should be considered. Furthermore, the band at 24 587 cm^{-1} (Fig. 8 in Ref. 13) shows intensity features very similar to the ones of the $^3T_2$ band (Fig. 5 in Ref. 13), both of them different than those of the a^3T_1 band (Fig. 9 in Ref. 13). In consequence, the assignment of the 24 587 cm^{-1} peak to the $A_1(^1A_1)$ component suggested by our energy calculations does not seem unreasonable from the point of view of intensity analysis, while its assignment as the E component of the b^3T_1 cannot be justified by intensity arguments exclusively. We must note that Campochiaro *et al.* claim inadequacy of the theoretical model used for the intensity calculations and comment several inconsistent results, such as the fact that the $^1T_2$ was precited to have the highest intensity of any of the ligand field transitions. We should join their suggestion for the need of more sophisticated theoretical studies. We think that the present work goes in that direction, at least in what respects to the energy features of the spectrum, and that theoretical efforts on intensity calculations are indeed needed.

IV. CONCLUSIONS

An *ab initio* theoretical study of the optical absorption spectrum of Ni^{2+}-doped MgO has been conducted by means of calculations in a MgO-embedded $(NiO_6)^{10-}$ cluster. The calculations include long- and short-range lattice embedding effects of electrostatic and quantum nature brought about by the MgO crystalline lattice as well as electron correlation and spin–orbit effects within the $(NiO_6)^{10-}$ cluster. The spin–orbit calculations have been performed with the recently proposed WB-AIMP method,[36] this being its first application to the field of doped crystals. The WB-AIMP method, which is based on spin–orbit-CI calculations,[39] has been extended here in order to be able to correct for those correlation effects which could be necessary in order to produce proper energy differences between spin-free states while unnecessary for the proper calculation of spin–orbit couplings. This extension of the WB-AIMP method, which is also aimed at keeping the size of the spin–orbit-CI within reasonable limits, is based on the use of spin-free-state shifting operators.

The results of the ligand field spectrum of $MgO:Ni^{2+}$ show a good overall agreement with the experimental measurements, both in the broad band transitions (spin-free) and in their spin–orbit components. The spin–orbit splittings are overestimated with the present method, but within reasonable limits, the resulting image being coherent in the ordering of states and in their relative separations, in spite of the fact that many of them are compressed in narrow energy windows. The fact that the *ab initio* results presented here lead to a balanced description of the whole set of spin–orbit ligand field states allows us to suggest that the existing assignment of the $E(b^3T_1)$ state should be reconsidered as the $A_1(^1A_1)$ one; the consistency of this suggestion with available intensity calculations has been discussed.

ACKNOWLEDGMENTS

This work was partly supported by grants from MEC (DGICYT PS92-0146) and Comunidad de Madrid (AE00276/95) Spain.

[1] W. Low, Phys. Rev. **109**, 247 (1958).
[2] R. Pappalardo, D. L. Wood, and J. R. C. Linares, J. Chem. Phys. **35**, 1460 (1961).
[3] J. E. Ralph and M. G. Townsend, J. Chem. Phys. **48**, 149 (1968).
[4] J. E. Ralph and M. G. Townsend, J. Phys. C **3**, 8 (1970).
[5] N. B. Manson, Phys. Rev. B **4**, 2645, 2656 (1971).
[6] W. E. Vehse, K. H. Lee, S. I. Yun, and W. A. Sibley, J. Luminiscence **10**, 149 (1975).
[7] M. V. Iverson and W. A. Sibley, J. Luminiscence **20**, 311 (1979).
[8] S. A. Payne, Phys. Rev. B **41**, 6109 (1990).
[9] R. J. Tonucci, S. M. Jacobsen, and W. M. Yen, Phys. Rev. B **43**, 7377 (1991).
[10] B. D. Bird, G. A. Osborne, and P. J. Stephens, Phys. Rev. B **5**, 1800 (1972).
[11] R. Moncorgé and T. Benyattou, Phys. Rev. B **37**, 9186 (1988).
[12] J. Koetke, K. Petermann, and G. Huber, J. Luminiscence **60&61**, 197 (1994).
[13] C. Campochiaro, D. S. McClure, P. Rabinowitz, and S. Dougal, Phys. Rev. B **43**, 14 (1991).
[14] M. J. L. Sangster and C. W. McCombie, J. Phys. C **3**, 1498 (1970).
[15] Z. Wen-Chen, Phys. Rev. B **40**, 7292 (1989).
[16] J. Sztucki, M. Daoud, and M. Kibler, Phys. Rev. B **45**, 2023 (1992).
[17] *Tunable Solid-State Lasers, Springer Series in Optical Science*, Vol. 47 edited by P. Hammerling, A. B. Budgor, and A. Pinto (Springer, Berlin, 1985).
[18] L. Seijo and Z. Barandiarán, Int. J. Quantum Chem. (to be published).
[19] S. R. Langhoff and C. W. Bauschlicher, Ann. Rev. Phys. Chem. **39**, 181 (1988).
[20] L. Seijo, Z. Barandiarán, and L. G. M. Pettersson, J. Chem. Phys. **98**, 4041 (1993).
[21] J. L. Pascual, L. Seijo, and Z. Barandiarán, J. Chem. Phys. **103**, 4841 (1995).
[22] S. López-Moraza, J. L. Pascual, and Z. Barandiarán, J. Chem. Phys. **103**, 2117 (1995).
[23] B. K. Teo, in *EXAFS Spectroscopy, Technique and Applications*, edited by B. K. Teo and D. C. Joy (Plenum, New York, 1981), p. 13.
[24] S. López-Moraza and Z. Barandiarán, J. Chem. Phys. **105**, 50 (1996).
[25] Z. Barandiarán and L. Seijo, J. Chem. Phys. **89**, 5739 (1988).
[26] J. L. Pascual, L. Seijo, and Z. Barandiarán, J. Chem. Phys. **98**, 9715 (1993).
[27] J. L. Pascual and L. Seijo, J. Chem. Phys. **102**, 5368 (1995).
[28] Z. Barandiarán and L. Seijo, in *Computational Chemistry: Structure, Interactions and Reactivity*, Vol. 77B of *Studies in Physical and Theoretical Chemistry*, edited by S. Fraga (Elsevier, Amsterdam, 1992), pp. 435–461.
[29] B. O. Roos, P. R. Taylor, and P. E. M. Siegbahn, Chem. Phys. **48**, 157 (1980); P. E. M. Siegbahn, A. Heiberg, J. Almlöf, and B. O. Roos, J. Chem. Phys. **74**, 2384 (1981); P. Siegbahn, A. Heiberg, B. Roos, and B. Levy, Phys. Scr. **21**, 323 (1980).
[30] R. Ahlrichs, P. Scharf, and C. Ehrhardt, J. Chem. Phys. **82**, 890 (1985); R. J. Gdanitz and R. Ahlrichs, Chem. Phys. Lett. **143**, 413 (1988).
[31] R. D. Cowan and D. C. Griffin, J. Opt. Soc. Am. **66**, 1010 (1976).
[32] Z. Barandiarán, L. Seijo, and S. Huzinaga, J. Chem. Phys. **93**, 5843 (1990).
[33] Z. Barandiarán and L. Seijo, Can. J. Chem. **70**, 409 (1992).
[34] J. H. Wood and A. M. Boring, Phys. Rev. B **18**, 2701 (1978).
[35] S. Katsuki and S. Huzinaga, Chem. Phys. Lett. **147**, 597 (1988); S. Huzinaga, J. Mol. Struct. (Theochem) **80**, 51 (1991).

[36] L. Seijo, J. Chem. Phys. **102**, 8078 (1995); M. Casarrubios and L. Seijo, Chem. Phys. Lett. **236**, 510 (1995).
[37] C. Teichteil, M. Pelissier, and F. Spiegelmann, Chem. Phys. **81**, 273 (1983).
[38] W. C. Ermler, Y. S. Lee, P. A. Christiansen, and K. S. Pitzer, Chem. Phys. Lett. **81**, 70 (1981).
[39] R. M. Pitzer and N. W. Winter, J. Phys. Chem. **92**, 3061 (1988).
[40] R. McWeeny, Proc. R. Soc. London, Ser. A **253**, 242 (1959); Rev. Mod. Phys. **32**, 335 (1960); M. Kleiner and R. McWeeny, Chem. Phys. Lett. **19**, 476 (1973); R. McWeeny, *Methods of Molecular Quantum Mechanics* (Academic, London, 1989).
[41] S. Huzinaga and A. A. Cantu, J. Chem. Phys. **55**, 5543 (1971); S. Huzinaga, D. McWilliams, and A. A. Cantu, Adv. Quantum Chem. **7**, 187 (1973).
[42] B. G. Dick and A. W. Overhauser, Phys. Rev. **112**, 90 (1958).
[43] S. Huzinaga, Z. Barandiarán, L. Seijo, and M. Klobukowski, J. Chem. Phys. **86**, 2132 (1987).
[44] R. W. G. Wyckoff, *Crystal Structures* (Wiley, New York, 1963).
[45] Detailed core and embedding AIMP data libraries in electronic format are available from the authors upon request or directly at the address http://sara.qfa.uam.es/Data/AIMPLibs.html.
[46] O. Gropen, M. Sjøvoll, H. Strømsnes, E. Karlsen, O. Swang, and K. Faegri, Jr., Theor. Chim. Acta **87**, 373 (1994).
[47] H. M. Evjen, Phys. Rev. **39**, 675 (1932).
[48] A. J. H. Wachters, J. Chem. Phys. **52**, 1033 (1970).
[49] P. J. Hay, J. Chem. Phys. **66**, 4377 (1977).
[50] L. G. M. Pettersson (private communication).
[51] T. H. Dunning and P. J. Hay, in *Modern Theoretical Chemistry*, edited by H. F. S. III (Plenum, New York, 1977).
[52] K. Pierloot and L. G. Vanquickenborne, J. Chem. Phys. **93**, 4154 (1990).
[53] MOLCAS version 2, K. Andersson, M. R. A. Blomberg, M. P. Fülscher, V. Kellö, R. Lindh, P.-Å. Malmqvist, J. Noga, J. Olsen, B. O. Roos, A. J. Sadlej, P. E. M. Siegbahn, M. Urban, P.-O. Widmark, University of Lund, Sweden (1992).
[54] ECPAIMP is an integral program for ECP and AIMP calculations written by L. G. M. Pettersson, L. Seijo, and M. A. Nygren.
[55] K. Pierloot, E. Tsokos, and B. O. Roos, Chem. Phys. Lett. **214**, 583 (1993).
[56] J. Miralles, O. Castell, R. Caballol, and J. P. Malrieu, Chem. Phys. **172**, 33 (1993).
[57] COLUMBUS suite of programs. (ARGOS, CNVRT, SCFPQ, LSTRN, CGDBG, and CIDBG.) R. M. Pitzer (principal author). See: A. H. H. Chang and R. M. Pitzer, J. Am. Chem. Soc. **111**, 2500 (1989), and references therein for a description. CNVRT and LSTRN have been adapted to handle ECPAIMP integrals by L. Seijo.